14. Jackson, J. D. *Classical Electrodynamics* (Wiley, New York, 1975).
15. Peebles, P. J. E. *Physical Cosmology* (Princeton University Press, 1971).
16. Owocki, S. P. & Rybicki, G. B. *Astrophys. J.* **284**, 337–350 (1984).
17. Lucy, L. B. *Astrophys. J.* **284**, 351–356 (1984).
18. Owocki, S. P., Castor, J. I. & Rybicki, G. B. *Astrophys. J.* **335**, 914–930 (1988).
19. Katz, J. I. *Astrophys. J.* **317**, 264–270 (1987).
20. Rees, M. J. *Mon. Not. R. astr. Soc.* **213**, 75P–81P (1985).
21. Sunyaev, R. A. & Zeldovich, Ya. B. *Ann. Rev. astr. Astrophys.* **18**, 537–560 (1980).
22. Zeldovich, Ya. B. & Novikov, I. D. *Relativistic Astrophysics: Volume 2, The Structure and Evolution of the Universe* (University of Chicago Press, 1983).
23. Rybicki, G. B. & Lightman, A. P. *Radiative Processes in Astrophysics* (Wiley, New York, 1979).
24. Peebles, P. J. E. *The Large Scale Structure of the Universe* (Princeton University Press, 1980).
25. Maddox, S. J. Efstathiou, G., Sutherland, W. J. & Loveday, J., *Mon. Not. R. astr. Soc* **242**, 43P–47P (1990).
26. Efstathiou, G. & Rees, M. J. *Mon. Not. R. astr. Soc.* **230**, 5P–11P (1988).
27. Hogan, C. J. & Kaiser, N. *Mon. Not. R. astr. Soc.* **237**, 31P–38P (1989).
28. Rubin, V. C. & Coyne, G. V. (eds) *Large Scale Motions in the Universe: A Vatican Study Week* (Princeton University Press, 1988).
29. Peebles, P. J. E. *Astrophys. J.* **153**, 1–11 (1968).
30. Krolik, J. *Astrophys. J.* **338**, 594–604 (1989).
31. Krolik, J. *Astrophys. J.* **353**, 21–23 (1990).
32. Lyubarsky, Y. E. & Sunyaev, R. A. *Astr. Astrophys.* **123**, 171–183 (1983).
33. Mather, J. *et al. Astrophys. J.* **354**, L37–L41 (1990).
34. Hogan, C. J. *Mon. Not. R. astr. Soc.* **202**, 1101–1126 (1983).
35. Bond, J. R., Carr, B. J. & Hogan, C. J. *Astrophys. J.* **367**, 420–454 (1991).
36. Hauser, M. G. *et al.* in *After the First Three Minutes*, Goddard Space Flight Center (in the press).
37. Wright, E. L. in *Proc. Texas-ESO-CERN Symposium*, New York Academy of Sciences (in the press).
38. Kashlinsky, A. & Jones, B. J. T. *Nature* **349**, 753–760 (1991).
39. Hogan, C. J. *Astrophys. J.* (submitted).

ACKNOWLEDGEMENTS. I am grateful for useful comments from M. Fukugita, J. P. Ostriker, M. J. Rees and H. Sato. This work was supported by grants from NASA and from the Alfred P. Sloan Foundation.

Regionally restricted developmental defects resulting from targeted disruption of the mouse homeobox gene *hox-1.5*

Osamu Chisaka & Mario R. Capecchi

Howard Hughes Medical Institute, Department of Human Genetics, University of Utah School of Medicine, Salt Lake City, Utah 84112, USA

Gene targeting in mouse embryo-derived stem cells has been used to disrupt the homeobox gene *hox-1.5*. Mice heterozygous at the *hox-1.5* locus appear normal, whereas *hox-1.5*$^{-}$/*hox-1.5*$^{-}$ mice die at or shortly after birth. These homozygotes are athymic, aparathyroid, have reduced thyroid and submaxillary tissue and exhibit a wide range of throat abnormalities. In addition, they often feature defects of the heart and arteries as well as craniofacial abnormalities. These deficiencies are remarkably similar to the pathology of the human congenital disorder DiGeorge's syndrome.

AN intriguing hypothesis is that a common set of genes, known as the homeobox genes, may be used in specifying the body plans of invertebrates and vertebrates alike. In *Drosophila* these genes, which include members of the Ultrabithorax and Antennapedia complexes, specify the identity of cells within each parasegment[1–3]. The function of the corresponding genes in man and mouse is not known, but as the order of these genes on the chromosomes of *Drosophila*, man and mouse is the same[4,5], and because this gene order reflects the order of anterior boundaries of gene expression along the anteroposterior body axis of the early embryos of all three species[6–8], it seems likely that these genes have an equally important role during mammalian development.

In man and mouse this set of genes, known collectively as the Hox genes, contains more than 30 members[9–11]. They are distributed in the genome in four separate linkage groups, Hox-1–4, on four different chromosomes. The four linkage groups are believed to have arisen during chordate evolution as the result of two duplications of chromosomal segments[12]. Expansion of this gene complex may have had a critical role in the progression from invertebrates to vertebrates by supplying the necessary complexity to this network of genes to accommodate the development of our complex body plan.

The homeobox genes of *Drosophila* encode transcription factors that share a DNA binding motif[13–15]. Molecular and genetic analyses have indicated that these genes act as master switches directing the course of morphogenic development of each segment[16–19]. As the human and mouse genes share similar homeobox sequences[20–22], the Hox proteins are thought to function also as transcription factors participating in the specification of regional information in the early mammalian embryo.

To determine the genetic function for some of the Hox genes in the mouse, we used gene targeting[23,24] in pluripotent mouse embryo-derived stem (ES) cells to create mice with specific mutations in these genes. We describe here the phenotype of mice that are homozygous for the disrupted *hox-1.5* gene.

Hox-1.5 is one of the earliest of the Hox genes to be expressed during mouse embryogenesis[25–29]. By *in situ* hybridization *hox-1.5* messenger RNA has been detected in presomitic mesoderm and in ectoderm of 7.5–8.0-day embryos. As embryogenesis progresses, the boundaries of *hox-1.5* expression sharpen and extend rostrally into the developing hind brain, anterior to the otic vesicles. At this stage, *hox-1.5* expression is strongest in neural ectoderm but can also be detected in prevertebral somites. By 12.5 days of gestation, after which the genesis of most organs in the mouse is well under way, *hox-1.5* expression is observed in a broad spectrum of organs and tissues including pharynx, aortic trunk, thyroid, spinal cord, spinal ganglia, lungs, stomach, spleen and kidneys.

Disruption of *hox-1.5* in ES cells

Figure 1*a* shows the targeting vector, pHox 1.5-N/TK1, TK2, used to disrupt the *hox-1.5* gene in ES cells. It contains 11.5 kilobases (kb) of mouse genomic sequence encompassing the *hox-1.5* locus, with the neomycin resistance (*neo*^{r}) gene from pMCIneopA (ref. 30) inserted into the *Bgl*II site within the *hox-1.5* homeobox domain[25]. Flanking the mouse sequences are the thymidine kinase genes, TK1 and TK2, isolated from herpes simplex virus (HSV) type I and II respectively. Two different HSV TK genes were used to construct this vector in order to reduce the potential for intraplasmid recombination. The linearized targeting vector was introduced into ES cells by electroporation[30] and the cells then grown in medium containing G418 plus gancyclovir to enrich for transformants containing the *neo*^{r} gene targeted into one of the endogenous *hox-1.5* loci[31]. Southern transfer analysis of DNA from G418 and gancyclovir-resistant colonies identified ES colonies that carry targeted disruptions of *hox-1.5*. One of 41 G418, gancyclovir-resistant colonies tested was positive. Figure 1*b* shows Southern blots of

DNA from the parental ES cell line, CC1.2 (ref. 32), and from the targeted ES cell line, 51-8, that were hybridized with DNA that flanks the *hox-1.5* gene (probe A) and is not present in the targeting vector, as well as with a *neo*^{r} probe (probe B). Cell line 51-8 is heterozygous at the *hox-1.5* locus, containing one copy of the mutated, *neo*^{r} disrupted allele, and one copy of the normal allele (Fig. 1*b*). In addition, 51-8 DNA was analysed using a *hox-1.5* genomic 5′ flanking probe (probe C, data not shown) which showed no additional rearrangements of the targeted locus either 5′ or 3′ of the *neo*^{r} insertion.

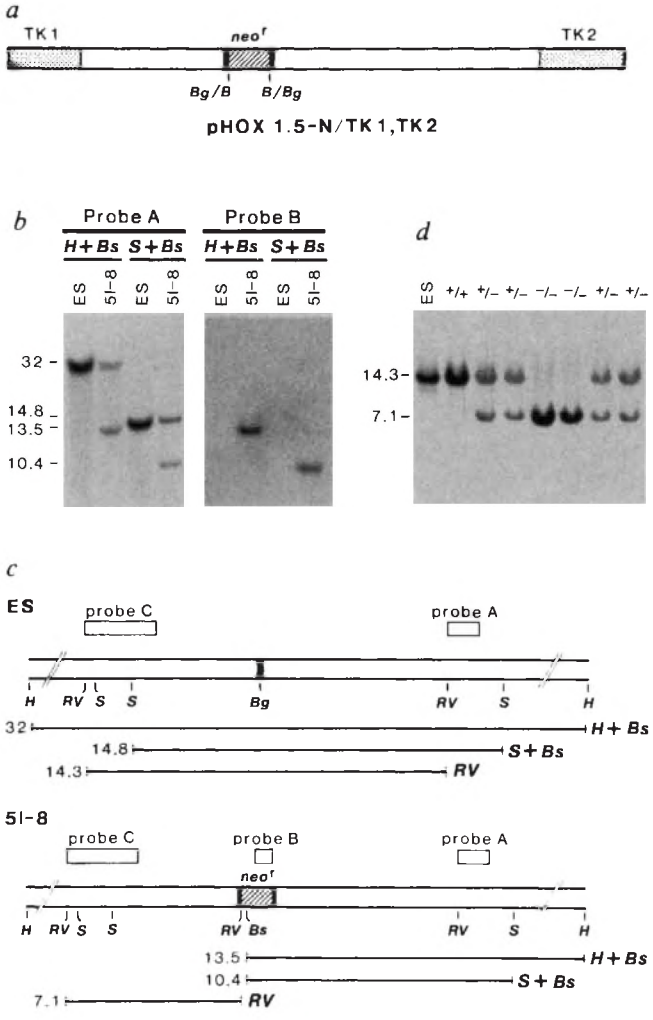

FIG. 1 Southern transfer analysis of ES cell line 51-8 containing a targeted disruption in the *hox-1.5* gene (*a*, *b* and *c*) and genotypic analysis of progeny derived from a *hox-1.5*$^-$/*hox-1.5*$^+$ intercross (*d*). *a*, Structure of the targeting vector, pHox 1.5-N/TK1, TK2, used to disrupt the *hox-1.5* gene in ES cells. *b*, Southern blot analysis of DNA from the parental ES cell line CCI.2 (ref. 32) and the targeted ES cell line, 51-8. The sizes of the DNA fragments are indicated in kb. The DNA samples were digested with *Hpa*I (*H*) and *Bst*BI (*Bs*), or with *Sac*I (*S*) and *Bst*BI, electrophoresed through agarose, transferred to nitrocellulose and hybridized with radioactively labelled probe as previously described[30]. Probe A is a 3′ *hox-1.5* genomic flanking probe, not present in the targeting vector (that is, a 1.2-kb *Eco*RV–*Cla*I fragment, see map in *c*. Probe B is a 0.6-kb, *Pst*I–*Bam*HI *neo*^{r} fragment and probe C is a 5′ *hox-1.5* genomic flanking probe (a 2.8-kb *Eco*RV–*Eco*RI fragment). *c*, Restriction map of the DNA fragments present in the parental and targeted ES cell lines CC1.2 and 51-8 respectively. *d*, Genotype, as determined by Southern transfer analysis, of 13.5-day-old embryos from interbreeding of *hox-1.5*$^-$ heterozygous mice. DNA was extracted from the yolk sac surrounding each embryo and analysed. DNA was digested with *Eco*RV and hybridized with flanking probe C. The genotype at the *hox-1.5* locus is indicated above each lane. +/+, Wild type; +/−, heterozygous at *hox-1.5*; −/−, homozygous for the *hox-1.5*$^-$ allele. ES represents a control lane of DNA from the parental CC1.2. The light hybridizing band migrating a little faster than the 14.3-kb fragment in the ES lane represents an *Eco*RV *hox-1.5* polymorphism present in the STO cell line used as a feeder cell line to propagate the ES cells. Bg, *Bgl*II; B, *Bam*HI; H, *Hpa*I; Bs, *Bst*BI; RV, *Eco*RV; S, *Sac*I.

Chimaeric mice were generated by microinjecting 51-8 cells (agouti coat colour) into blastocysts derived from C57Bl/6 mice (nonagouti coat colour), followed by surgical transfer of the blastocysts into the uteri of pseudopregnant mice. Seven chimaeric mice were born, all of which were males with >80% agouti coats. Test breeding of the chimaeric males to C57Bl/6 females showed that three of these animals transmitted the ES-derived agouti coat colour to their offspring. All of the offspring of one of the chimaeric males were agouti, whereas the others sired agouti offspring at a frequency of 20% to 30%. The frequency of generating germ-line chimaeras with the 51-8 cell line was comparable to that obtained with the parental cell line CC1.2.

Mice heterozygous for the *hox-1.5*$^-$ mutation are fertile and appear normal. The *hox-1.5* genotype of siblings, derived from intercrosses of *hox-1.5* heterozygotes, were evaluated by Southern transfer analysis of tail DNA obtained from newborn mice or from DNA extracted from the yolk sac surrounding each embryo. Figure 1*d* shows a representative analysis of such a litter at 13.5 days of gestation. All three genotypes expected were present.

Hox-1.5$^-$/*hox-1.5*$^-$ mice do not die *in utero*. Of 150 mid-to-late gestation embryos analysed for genotype, 36 were homozygous for the wild-type allele, 77 were heterozygotes and 37 were homozygous for the mutant allele. The apparent 1:2:1 segregation of *hox-1.5* alleles among these embryos suggests that *hox-1.5*$^-$/*hox-1.5*$^-$ embryos are not preferentially aborted or absorbed.

Phenotype of newborn *hox-1.5*$^-$/*hox-1.5*$^-$ mice

Mice containing two defective copies of the *hox-1.5* gene die at or shortly after birth, the longest period of survival being 12 h. Those that survived birth were noticeably purple and apparently died from problems associated with circulation of the blood and/or pulmonary failure.

In about half (20/38) of the newborn *hox-1.5*$^-$/*hox-1.5*$^-$ mice the abdomen was bloated. After puncturing the abdominal wall, air rather than fluid was released; puncturing under water showed that air was present in the peritoneal cavity, in the stomach, and in the intestines.

Organ defects

The first feature apparent in embryos and newborn *hox-1.5*$^-$ homozygotes was an abnormal body shape. Figure 2 compares body shapes of control heterozygous (*a*, *b* and *c*) and homozygous (*d*, *e* and *f*) *hox-1.5*$^-$ mice at three different stages. Relative to their heterozygous litter mates, the homozygous *hox-1.5*$^-$ mice are much more rounded, their necks are shortened and their heads are characteristically tilted into their chests.

Examining sagittal and parasagittal sections of the 13.5- and 15.5-day embryos indicated that most *hox-1.5*$^-$/*hox-1.5*$^-$ mice were athymic (compare, for example, Fig. 2*b* and *e*). This was confirmed by examining sections from six newborn mutant mice. Figure 3 shows a sagittal section of the throat region from a *hox-1.5* heterozygous and a homozygous newborn mouse. The thymus is obviously absent in the section from the *hox-1.5*$^-$/*hox-1.5*$^-$ mouse. No thymus tissue was evident in any of the sagittal or parasagittal sections. In addition to the absence of thymus tissue, most of these newborn mice also lacked parathyroid tissue and the amount of thyroid tissue was greatly reduced. (In two mutant mice small amounts of thymic tissue could be detected, corresponding to the caudal tips of the thymic lobes.)

In the sections shown in Fig. 3*a* and *b*, it is also evident that the neck region of the *hox-1.5*$^-$/*hox-1.5*$^-$ mouse is noticeably shorter relative to the control *hox-1.5*$^-$ heterozygous mouse. For example, note the distance from the heart and superior vena cava to the thyroid gland in the *hox-1.5*$^-$/*hox-1.5*$^-$ mouse (Fig.

3*b*). At the same magnification of the throat, the thyroid, heart and superior vena cava from the *hox-1.5*$^-$ heterozygous mouse are not in the same photographic field (Fig. 3*a*).

The thoracic region of eight *hox-1.5*$^-$/*hox-1.5*$^-$ newborn mice was examined microscopically and/or histologically and compared with that from normal heterozygous and wild-type litter mates. A range of cardiovascular defects was observed. Two of the mice were missing the right carotid artery, and the size and shape of the compartments of the heart were abnormal in seven *hox-1.5*$^-$/*hox-1.5*$^-$ mice: this included dilation and thickening of the wall of the right atrium and left ventricle, as well as the right ventricle being smaller and having a thinner wall. Classical septal and transposition defects, including persistent truncus arteriosis, were not seen.

Figure 4 shows coronal sections from the thoracic region of a *hox-1.5*$^-$/*hox-1.5*$^-$ mouse (*a*, *b*, *d* and *f*) and a control *hox-1.5*$^-$ heterozygous litter mate (*c* and *e*). Hypertrophy of both atria is prominent in the mutant mouse (compare Fig. 4*c* and *d*). Figure 4*a* and *b* show persistent patent ductus arteriosis. Three mutant mice but no control litter mates had this condition. Further, the aorta in this *hox-1.5*$^-$/*hox-1.5*$^-$ mouse, as well as in three others, has a thin wall and is poorly developed (Fig. 4*c* and *d*). Stenosis of the aortic valve was also apparent. Figure 4*e* and *f* shows that this mouse has a defective pulmonary semilunar valve, containing two rather than the normal three cusps. This feature was observed in three *hox-1.5*$^-$/*hox-1.5*$^-$ mice.

The hypertrophy of the atria and the enlargement of all of the chief veins, including the jugular veins, the pulmonary veins and the superior and inferior vena cava (Fig. 4*a*, *b*, *d* and *f*) are strong indicators of cardiovascular dysfunction. In addition, the most likely cause for early death of the *hox-1.5*$^-$/*hox-1.5*$^-$ mice is cardiovascular dysfunction, although the details of the anatomical and physiological cause(s) for the cardiovascular dysfunction remain to be determined.

Although it is not apparent from the sections shown in Fig. 4, this *hox-1.5*$^-$/*hox-1.5*$^-$ mouse, as well as four others, had greatly reduced amounts of submaxillary tissue relative to normal litter mates.

Skeletal defects

To examine further the shortened neck of *hox-1.5*$^-$/*hox-1.5*$^-$ mice, trypsin/alkaline-cleared preparations of newborn mice were made and stained with alizarin red S and alcian blue to visualize the ossified bone and cartilage respectively[33]. The number of cervical vertebrae was the same in heterozygous and homozygous litter mates, but the positioning of bones in the neck was different. In the mutant mouse shown in Fig. 5*b*, the entire thoracic region of the mouse is thrust towards the head, and the end of the clavicle is at the level of the axis rather than at the level of two cervical vertebrae caudal to the axis. Also, the larynx and trachea are positioned much closer to the cervical vertebrae than in control mice (see Fig. 5*a*–*d*). Detailed examination of the structure of the larynx revealed that the lesser horn (cornu minus) of the hyoid bone is absent in *hox-1.5*$^-$/*hox-1.5*$^-$ mice (Fig. 5*c* and *d*). Also, the thyroid and cricoid cartilages are shorter and thicker in the mutant mouse. Facial features are also abnormal, due largely to the maxilla and mandible being shorter and altered in shape (see Fig. 5*a* and *b*). Measurements of the length of the mandible, relative to the height of the skull from four heterozygous and homozygous *hox-1.5* mice, indicated that this ratio was reduced by 6 ± 2% in the *hox-1.5*$^-$/*hox-1.5*$^-$ mice relative to the control litter mates. A further example of facial malformations is that the zygomatic process of the squamosal bone is altered in the *hox-1.5*$^-$ homozygous mouse (Fig. 5*e* and *f*).

Bloated phenotype

About half of the *hox-1.5*$^-$/*hox-1.5*$^-$ mice that survive birth have a bloated abdomen (Fig. 6*b*). To understand the cause of

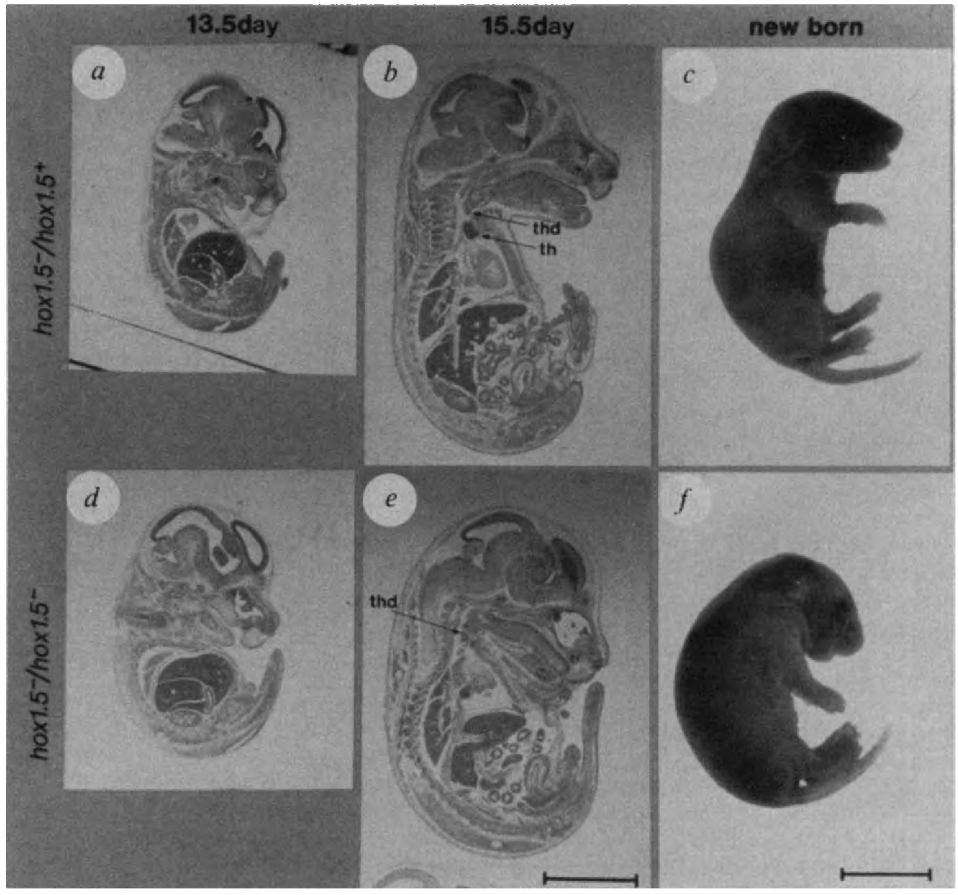

FIG. 2 Comparison of body shapes of *hox-1.5*$^-$ heterozygous (*a*, *b* and *c*) and homozygous (*d*, *e* and *f*) mice; *a*, *b*, *d* and *e* show parasagittal and sagittal sections of 13.5- and 15.5-day-old embryos respectively; *c* and *f* are photographs of newborn mice. Before sectioning, embryos were fixed in Bouin's reagent, embedded in paraffin and regressively stained with haematoxylin and eosin (H and E) as described[44]. The *hox-1.5*$^-$/*hox-1.5*$^-$ mice and embryos are more rounded, their necks shortened and their heads tilted into their chest, relative to control, *hox-1.5*$^-$/*hox-1.5*$^+$ heterozygous litter mates. thd, Thyroid; th, thymus. Scale bar in *a*, *b*, *d* and *e*, 5 mm; *c* and *f*, 6 mm.

the bloated phenotype, it is important to reexamine the throat region of the *hox-1.5*$^{-}$/*hox-1.5*$^{-}$ mice. In Fig. 6*d*–*i* we compare sagittal sections of the throat from heterozygous and homozygous *hox-1.5*$^{-}$ newborn mice. As with the cleared preparations, structural differences in the larynx and trachea are apparent in these sections. The shapes of the thyroid and cricoid cartilages are altered in the *hox-1.5*$^{-}$ homozygous mouse, and the larynx is narrower. In addition to structural differences in the cartilages, the musculature in the throat is not as well organized as in the heterozygote, as is evident in the disordered array of muscle fibres in the lower part of the tongue (Fig. 6*f* and *i*), the connections of the muscle to the epiglottis (Fig. 5*e*, *f*, *h* and *i*) and the muscles surrounding the oesophagus (Fig. 6*d* and *g*). In the control animal, but not the *hox-1.5*$^{-}$ homozygote, the entrance to the oesophagus is constricted (Fig. 5, compare *d* and *e* with *g* and *h*), the epiglottis is pulled back from the entrance to the trachea (Fig. 5, compare *e* and *f* with *h*) and the soft palate is positioned to favour passage of air from the nasal passage to the trachea. Although the *hox-1.5*$^{-}$/*hox-1.5*$^{-}$ mouse was breathing at the time of termination, the absence of control of the oesophagus and epiglottis may indicate a dysfunction in this musculature and/or neurons innervating these muscles. Similar structural malformations of the trachea and oesophagus are evident in the coronal sections of the *hox-1.5*$^{-}$/*hox-1.5*$^{-}$ mouse shown in Fig. 4. The trachea and bronchi in the *hox-1.5*$^{-}$ homozygous mouse are much smaller than those of the control (Fig. 4*d* and *f*). Note in particular that the oesophagus in the *hox-1.5*$^{-}$/*hox-1.5*$^{-}$ mouse (Fig. 4*d* and *f*) is not surrounded by a ring of muscle.

As previously mentioned, the stomach and intestines of *hox-1.5*$^{-}$/*hox-1.5*$^{-}$ mice were found to be full of air. Because of difficulties with breathing, perhaps compounded by heart and arterial defects and possible dysfunction of the air passages in the throat, the *hox-1.5*$^{-}$/*hox-1.5*$^{-}$ mice appear to pump air into their stomach and intestines. When the air pressure becomes sufficiently high, the lining of the stomach and/or intestine perforates, allowing leakage of air into the peritoneum. Similar pathology has been observed in human infants, where pumping of air into the stomach and intestines can result in perforation of their lining. This condition can be induced in human infants from the trauma associated with choking.

Structure of the pharyngeal arches

Many of the tissues and organs that are deficient in the *hox-1.5*$^{-}$/*hox-1.5*$^{-}$ mouse are derived from the pharyngeal arches and/or pharyngeal pouches. For example, the thymus and parathyroid are derived from cells in pharyngeal pouch 3 and 4, the carotid artery is derived from pharyngeal arch 3 and so on. Thus, it may be significant that the pattern of pharyngeal arches in the 10.5-day embryos is altered. The relative position and perhaps the size of pharyngeal arch 4 is different in 10.5-day embryos of heterozygous compared with homozygous mice, and the demarcation between pharyngeal arch 3 and 4 is less well defined (Fig. 7*a*–*d*).

Sagittal, coronal and transverse sections of four 10.5-day embryos were examined. The rhombomeric pattern in the developing hind brain in *hox-1.5*$^{-}$/*hox-1.5*$^{-}$ mutants appeared normal and all of the sensory and motor cephalic ganglia were also distinguishable and appeared histologically normal (data not shown).

Discussion

Gene targeting in mouse ES cells has been used to disrupt the *hox-1.5* homeobox gene. ES cells containing the disrupted *hox-1.5* gene were used to generate chimaeric mice that transmitted the mutant gene to their progeny, and intercrosses between mice heterozygous for the *hox-1.5*$^{-}$ mutation were used to generate *hox-1.5*$^{-}$/*hox-1.5*$^{-}$ mice. These mice exhibit a complex phenotype with multiple defects in thymus, parathyroid, thyroid and submaxillary glands, facial cartilages such as the maxilla and mandible, and the zygomatic process of the squamosal bone, hyoid, thyroid and cricoid cartilages, heart and great vessels issuing from the heart, carotid artery, soft palate, and connective and muscular tissues of the throat and tongue. Many of these defects are in tissues, cartilages and organs derived from all four pharyngeal arches and/or pouches. Thus, *hox-1.5* may play a critical part in the patterning of tissues in all of the pharyngeal arches and pouches. In addition, the spectrum of muscle deficiencies in the neck and tongue, as well as possible endothelial tissue deficiency in the aorta[34] may indicate that targets for *hox-1.5* include occipital myotomes, as well as the pharyngeal arch mesoderm that contributes to the muscle of the pharynx and larynx. Clearly, *hox-1.5* affects tissues and structures derived from multiple primary cell lineages.

Alternatively, or in addition, *hox-1.5* may be important for cephalic neural crest function. With the chick/quail chimaeric system[35–39], it has been shown that the proper formation of the affected tissues and organs requires interaction of cephalic neural crest with cells in the pharyngeal arches and pouches. In addition to possible inductive processes involving interactions between neural crest and pharyngeal ectoderm, mesoderm and endoderm cells, neural crest also may contribute directly to the affected tissues by providing connective tissues derived from mesenchymal neural crest. Interestingly, microablation of premigratory cephalic neural crest in early chick embryos has effects very similar to those reported here for the *hox-1.5*$^{-}$/*hox-1.5*$^{-}$ mouse, including loss of thymus, parathyroid and thyroid tissue, shortened necks, heart and arterial defects and alteration of pharyngeal arch architecture[40–42]. The experiments by Kirby and her coworkers concentrated on removing cephalic neural crest caudal to the otic vesicles. The additional craniofacial abnormalities in the *hox-1.5*$^{-}$/*hox-1.5*$^{-}$ mouse would argue that if the effect of the *hox-1.5*$^{-}$ mutation is at the level of cephalic neural crest, then the influence of *hox-1.5*$^{-}$ would also extend to neural crest cells rostral to the otic vesicles.

As *hox-1.5*$^{-}$ homozygous mice exhibit a specific phenotype it can be concluded that the other members of the *hox-1.5* subfamily (*hox-2.7*, *hox-3.6*, and *hox-4.1*) cannot fully complement the *hox-1.5* mutation. We can thus infer that the four clusters of closely related homeobox genes in vertebrates are not functionally redundant. Each member of the Hox complex may have a critical role in development. As a member of a network of genes, *hox-1.5* is likely to participate in cross regulation. One testable prediction of the above hypothesis is that the patterns of gene expression of other *hox* genes may differ in the *hox-1.5*$^{-}$/*hox-1.5*$^{-}$ mouse. Although the phenotype of the *hox-1.5*$^{-}$/*hox-1.5*$^{-}$ mouse is complex, it is nonetheless restricted with respect to the affected region of the mouse. Had the coupling between the Hox genes been extensive, then it might have been anticipated that the *hox-1.5*$^{-}$ mutation would have yielded an undecipherable early embryonic lethal phenotype. Instead, the *hox-1.5*$^{-}$/*hox-1.5*$^{-}$ mice are born with a fairly well defined set of deficiencies.

The sequence of *hox-1.5* is most closely related to the *Drosophila* antennapedia complex genes Zerknullt (*zen*) and proboscipidia (*pb*). *Zen* is unique among this cluster of genes in that it seems not to be involved in the process of anteroposterior segmentation but rather in dorsal-ventral patterning[43]. *Pb*, on the other hand, is involved in anteroposterior patterning and is required for differentiation of adult labial and maxillary structures[44]. Loss of *pb* function transforms adult mouth parts to legs. The phenotypes associated with the loss of *hox-1.5* function in the mouse do not appear to involve transformations. Rather, as we have described, the loss of *hox-1.5* function most commonly affects the form of structures in a given region of the mouse and in this respect the *hox-1.5* gene seems to be required for regional refinement of pattern rather than for the establishment of pattern *per se*. The multiplicity of Hox genes in vertebrates may therefore be functionally correlated with developmental refinement of the more complex form

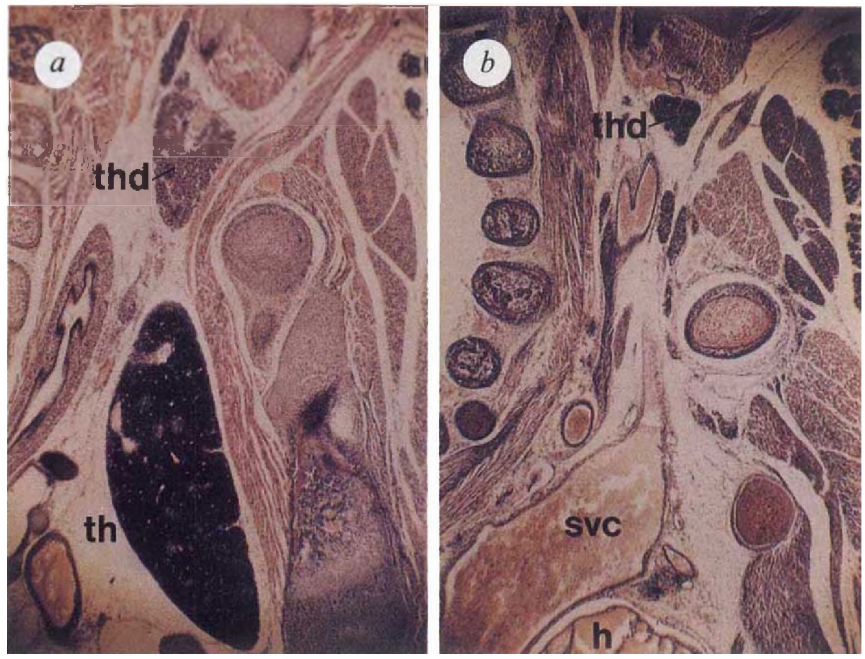

FIG. 3 *Hox-1.5*$^{-}$*/hox-1.5*$^{-}$ mice are usually athymic. Sagittal sections of the throat region from a *hox-1.5*$^{-}$ heterozygous (*a*) and homozygous (*b*) mouse are shown. No thymus or parathyroid tissue could be detected in this *hox-1.5*$^{-}$*/hox 1.5*$^{-}$ mouse. After fixing and embedding in paraffin, the entire mouse was sectioned into 10-μm sections and every fourth section was examined. The amount of thyroid tissue present in this mutant mouse is also greatly reduced. thd, Thyroid; th, thymus; svc, superior vena cava; h, heart. The width of *a* or *b* corresponds to 2.5 mm.

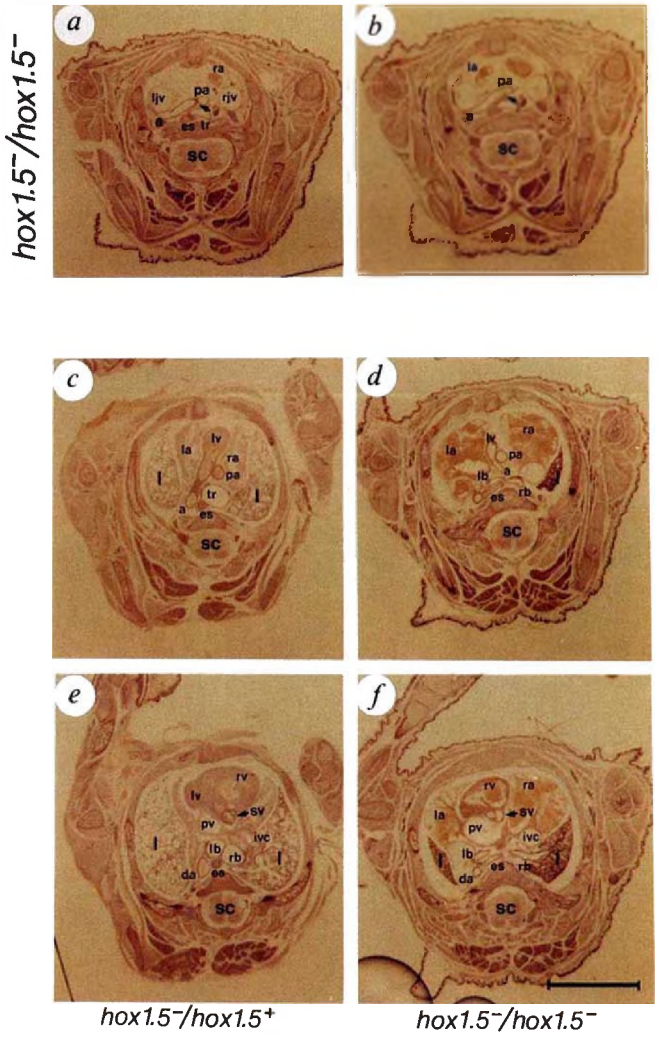

FIG. 4 Heart and arterial defects in the *hox-1.5*$^{-}$*/hox-1.5*$^{-}$ mouse. Coronal sections from the thoracic region of *hox-1.5*$^{-}$ heterozygous (*c* and *d*) and homozygous (*a*, *b*, *d* and *f*) mice are shown; *a* and *b* show persistent patent ductus arteriosis (see arrows); *c* and *d* compare the aorta as it leaves the left ventricle in a control *hox-1.5*$^{-}$ heterozygous mouse (*c*), and in a mutant *hox-1.5*$^{-}$*/hox-1.5*$^{-}$ mouse (*d*). Note that the aorta has a thin wall and is poorly developed in the mutant mouse; *e* and *f* show a coronal section through the pulmonary semilunar valve of a *hox-1.5*$^{-}$ heterozygous (*e*) and homozygous (*f*) mouse. Note that this valve in the mutant mouse contains two, rather than the normal three, cusps, and the hypertrophy of the left and right atria as well as the enlargement of all the main veins in the mouse. a, Aorta; pa, pulmonary artery; da, descending aorta; la, left atrium; ra, right atrium; lv, left ventricle; rv, right ventricle; sv, semilunar valve; es, oesophagus; tr, trachea; rb, right bronchus; lb, left bronchus; sc, spinal cord; ljv, left jugular vein; rjv, right jugular vein; pv, pulmonary vein; svc, superior vena cava; ivc, inferior vena cava; l, lungs. Scale bar, 3.5 mm.

of vertebrates.

The reported pattern of *hox-1.5* gene expression in mouse embryos does not correlate in any simple way with the pattern of defects we have observed in mice with mutated *hox-1.5* genes. The genetic function of *hox-1.5*, as defined here, is more spatially and temporally restricted than the gene expression pattern would predict. *hox-1.5* is expressed in the lungs, stomach, spleen and kidneys[25-29]; however, no mutant phenotype can be detected in these organs. The lungs in *hox-1.5*$^{-}$/*hox-1.5*$^{-}$ mice may not function normally, but this seems likely to result from a secondary consequence of poor circulation of blood or premature death as judged by light microscopy. The size, shape and tissue quality of the lungs appear normal during development and in newborn mutant mice. What may be critical for correlating the

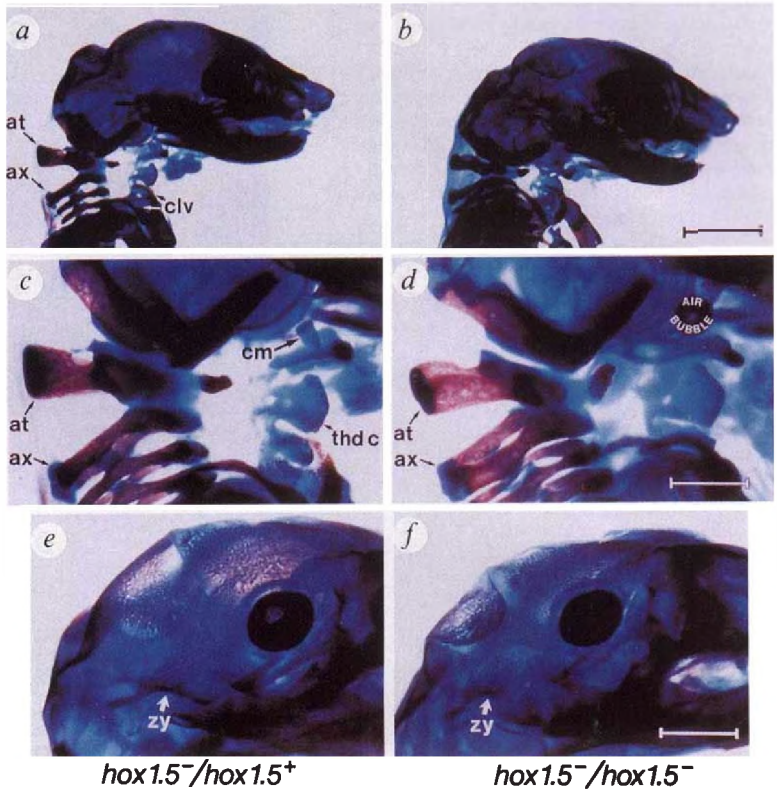

FIG. 5 Comparison of skeletons from *hox-1.5*$^{-}$ heterozygous (*a*, *c* and *e*) and homozygous (*b*, *d* and *f*) mice. Newborn mice were cleared by treatment with trypsin and KOH and stained with alizarin red S and alcian blue to visualize the ossified bone and cartilage respectively[33]. *a* and *b*, Head and neck regions. The whole thoracic region in the mutant mouse (*b*) is thrust towards the head, and the larynx is positioned closer to the cervical vertebrae compared with the control heterozygous *hox-1.5*$^{-}$ mouse (*a*). In the lower jaw, the mandible also appears shorter and is thicker in the *hox-1.5*$^{-}$/*hox-1.5*$^{-}$ mouse. *c* and *d*, Detail of the hyoid bone and thyroid cartilage. In the *hox-1.5*$^{-}$/*hox-1.5*$^{-}$ mouse the lesser horn of the hyoid bone (cornu minus, cm) is missing. *e* and *f*, Zygometric process of the squamosal bone (zy) is altered in shape in the *hox-1.5*$^{-}$/*hox-1.5*$^{-}$ mouse (*f*). at, Atlas; ax, axis; clv, clavicle; cm, carnu minus; thdc, thyroid cartilage; zy, zygomatic process of the squamosal bone. The bar represents 2 mm in *a* and *b*, but 1 mm in *c*–*f*.

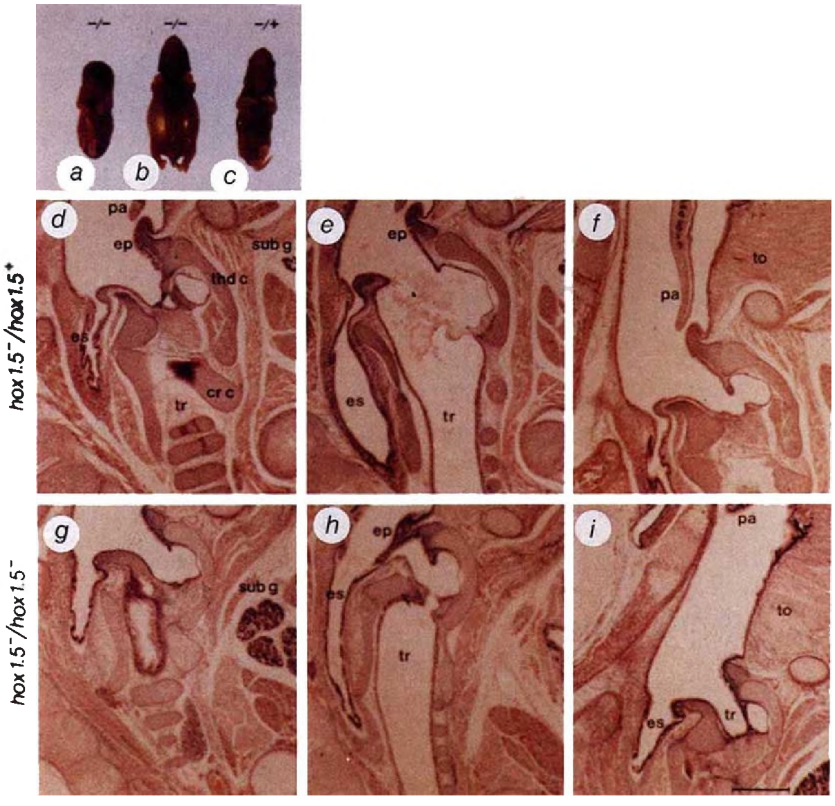

FIG. 6 Bloated phenotype and detail of the oesophagus and trachea. Photographs of newborn mice; *a*, a *hox-1.5*$^{-}$/*hox-1.5*$^{-}$ mouse that was dead at birth; *b*, a *hox-1.5*$^{-}$/*hox-1.5*$^{-}$ mouse that survived birth and developed a bloated abdomen; *c*, control *hox-1.5*$^{-}$ heterozygous mouse. Sagittal sections that detail the throat region; *d*–*f* are sagittal sections from a heterozygous *hox-1.5*$^{-}$ mouse; *g*–*i* are sagittal sections from a *hox-1.5*$^{-}$/*hox-1.5*$^{-}$ mouse. Both mice survived birth and were breathing at the time of termination. In the control *hox-1.5*$^{-}$/*hox-1.5*$^{+}$ mouse the entrance to the oesophagus is constricted (*d* and *e*), the epiglottis is pulled back (*d*, *e* and *f*) and the soft palate is positioned to allow air from the nasal passage to enter the trachea. In the *hox-1.5*$^{-}$/*hox-1.5*$^{-}$ mouse the entrance to the oesophagus is not constricted (*g*, *h* and *i*), the epiglottis is not pulled back (*h*) and the soft palate is truncated so that it does not favour the nasal or mouth passages. The organization of the muscle surrounding the oesophagus, connecting to the epiglottis, and in the back of the tongue are poorly organized in the *hox-1.5*$^{-}$/*hox-1.5*$^{-}$ mouse. pa, soft palate; ep, epiglottis; subg, submaxillary gland; thdc, thyroid cartilage; crc, cricoid cartilage; es, oesophagus; tr, trachea; to, tongue. The length of the bar in *d*–*i* represents 0.5 mm.

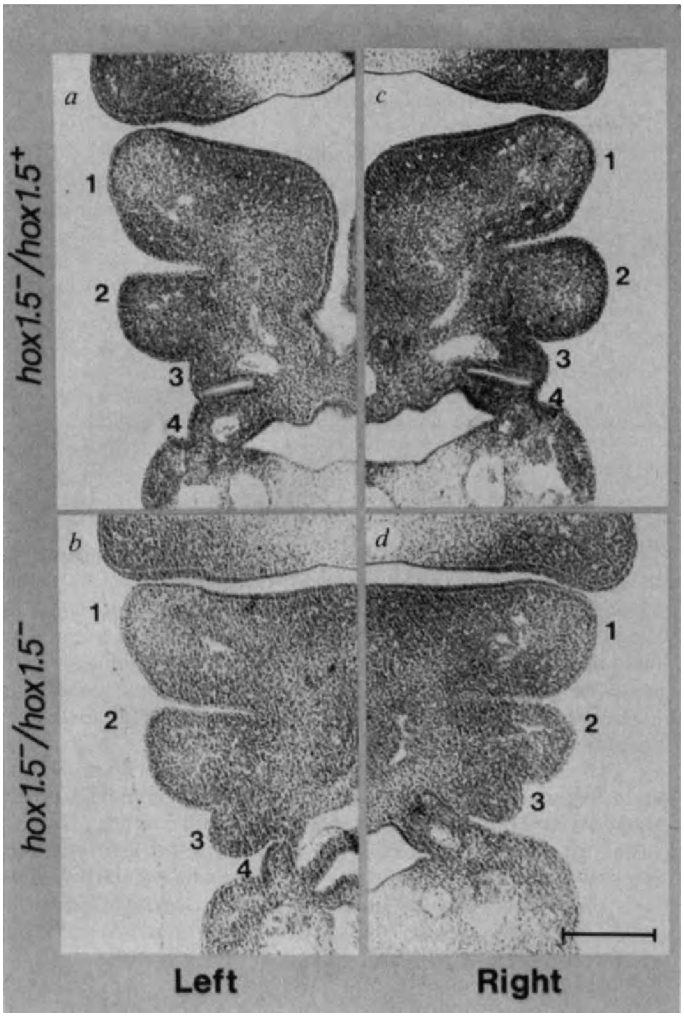

FIG. 7 Pharyngeal arches from *hox-1.5*$^-$ heterozygous (*a* and *c*) and homozygous (*b* and *d*) mice. Coronal sections of 10.5-day-old mouse embryos illustrating the left (*a* and *b*) and right (*c* and *d*) pharyngeal arches. In the *hox-1.5*$^-$/*hox-1.5*$^-$ mouse, the left (*b*) and right (*d*) pharyngeal arch 4 is displaced. Also the demarcation between pharyngeal arches 3 and 4 is not as well defined in the *hox-1.5*$^-$/*hox-1.5*$^-$ mouse. Scale bar, 0.3 mm.

gene expression pattern with the mutant phenotype is the anterior portion of *hox-1.5* gene expression. A similar correlation was also observed in *int-1*$^-$/*int-1*$^-$ mice[45,46]. Although *int-1* is expressed along the entire neural plate, from the mid brain to the caudal tip of the neural tube, phenotypic consequences of disrupting *int-1* were only apparent in the rostral portion of this expression pattern (that is, corresponding to the mid-brain and the anterior portion of the hind brain). The spinal cord, for example, was normal in the *int-1*$^-$/*int-1*$^-$ mice.

Humans with the congenital deficiency DiGeorge' syndrome are athymic, aparathyroid, have reduced thyroid tissue, bear craniofacial abnormalities and often are afflicted with cardiac and arterial defects[47]. The coincidence of this set of deficiencies with those observed in the *hox-1.5*$^-$/*hox-1.5*$^-$ mouse is remarkable, although important differences exist between the human and mouse syndrome. DiGeorge's syndrome is autosomal dominant, whereas the mouse *hox-1.5*$^-$ phenotype is autosomal recessive. DiGeorge's syndrome has been associated with deletions and translocations involving chromosome 22, whereas the human homologue to *hox-1.5* maps to chromosome 7. But as most patients with DiGeorge's syndrome are karyotypically normal[48], it is possible that the DiGeorge's syndrome phenotype could result from mutations in separate genes. Irrespective of whether or not the DiGeorge's syndrome phenotype of some patients can be attributed to mutations in the human *hox-1.5* gene, the similarity of phenotype in man and mouse argues for a common developmental pathway. In this context, the *hox-1.5*$^-$ mouse may prove to be a useful model for DiGeorge's syndrome. □

Received January 31; accepted 7 March 1991.

1. Lewis, E. B. *Nature* **276,** 565–570 (1978).
2. Kaufman, T. C., Lewis, R. & Wakimoto, B. *Genetics* **94,** 115–133 (1980).
3. Bender, W. *et al. Science* **221,** 23–29 (1983).
4. Holland, P. W. H. & Hogan, B. L. M. *Genes Dev.* **2,** 773–782 (1988).
5. Kessel, M. & Gruss, P. *Science* **249,** 374–379 (1990).
6. Harding, K., Wedeen, C., McGinnis, W. & Levine, M. *Science* **229,** 1236–1242 (1985).
7. Duboule, D. & Dolle, P. *EMBO J.* **8,** 1497–1505 (1989).
8. Graham, A., Papalopulu, N. & Krumlauf, R. *Cell* **57,** 367–378 (1989).
9. Acampora, D. *et al. Nucleic Acids Res.* **17,** 10385–10401 (1989).
10. Duboule, D. *et al. Genomics* **7,** 458–459 (1990).
11. Martin, G. *et al. Nature* **325,** 21 (1987).
12. Kappen, C., Schughart, K. & Ruddle, F. H. *Proc. natn. Acad. Sci. U.S.A.* **86,** 5459–5463 (1989).
13. McGinnis, W., Garber, R. L., Wing, J., Kurowia, A. & Gehring, W. J. *Cell* **37,** 403–408 (1984).
14. McGinnis, W., Levine, M. L., Hafen, E., Kurowia, A. & Gehring, W. J. *Nature* **308,** 428–433 (1984).
15. Scott, M. P. & Weiner, A. J. *Proc. natn. Acad. Sci. U.S.A.* **81,** 3115–3119 (1984).
16. Nusslein-Volhard, C. & Wieschaus, E. *Nature* **287,** 795–801 (1980).
17. Akam, M. *Development* **101,** 1–22 (1987).
18. Gehring, W. J. *Science* **236,** 1245–1252 (1987).
19. Ingham, P. W. *Nature* **335,** 25–34 (1988).
20. Carrasco, H. E., McGinnis, W., Gehring, W. J. & DeRobertis, E. M. *Cell* **37,** 409–414 (1984).
21. McGinnis, W., Hert, C. P., Gehring, W. J. & Ruddle, F. M. *Cell* **38,** 675–680 (1984).
22. Scott, M. P., Tamkum, J. W. & Hartzell, G. W. *Biochim. Biophys. Acta* **989,** 25–48 (1989).
23. Capecchi, M. R. *Trends Genet.* **5,** 70–76 (1989).
24. Capecchi, M. R. *Science* **244,** 1288–1292 (1989).
25. Gaunt, S. L., Miller, J. R., Powell, D. J. & Duboule, D. *Nature* **324,** 662–664 (1986).
26. Fainsod, A., Awgulewitsch, A. & Ruddle, F. H. *Devl. Biol.* **124,** 125–133 (1987).
27. Gaunt, S. L. *Development* **101,** 51–60 (1987).
28. Gaunt, S. L., Sharpe, P. T. & Duboule, D. *Development Suppl.* **104,** 169–179 (1988).
29. Gaunt, S. J. *Development.* **103,** 135–144 (1989).
30. Thomas, K. R. & Capecchi, M. R. *Cell* **51,** 503–512 (1987).
31. Mansour, S. L., Thomas, K. R. & Capecchi, M. R. *Nature* **336,** 348–352 (1988).
32. Bradley, A., Evans, M., Kaufman, M. H. & Robertson, E. *Nature* **309,** 255–256 (1984).
33. McLeod, M. J. *Teratology* **22,** 299–301 (1980).
34. Noden, D. M. *Ann. N.Y. Acad. Sci.* **588,** 236–249 (1990).
35. LeLevre, C. S. & LeDouarin, N. M. *J. Embryol. exp. Morph.* **34,** 125–154 (1975).
36. LeDouarin, N. *The Neural Crest* (Cambridge Univ. Press, 1980).
37. Couly, G. & LeDouarin, N. M. *Development Suppl.* **103,** 101–113 (1988).
38. Noden, D. M. *Devl. Biol.* **42,** 106–130 (1975).
39. Noden, D. M. *Development Suppl.* **103,** 121–140 (1988).
40. Kirby, M. L., Gall, T. F. & Stewart, D. E. *Science* **220,** 1059–1061 (1983).
41. Bockman, D. E. & Kirby, M. *Science* **22,** 498–500 (1984).
42. Bockman, D. E., Redmond, M. E. & Kirby, M. L. *Anat. Rec.* **225,** 209–217 (1989).
43. Rushlow, C., Doyle, H., Hoey, T. & Levine, M. *Genes Dev.* **1,** 1268–1279 (1987).
44. Pultz, M. A., Diederich, R. J., Gribbs, D. L. & Kaufman, T. C. *Genes Dev.* **2,** 901–920 (1988).
45. Thomas, K. R. & Capecchi, M. R. *Nature* **346,** 847–850 (1990).
46. McMahon, A. P. & Bradley, A. *Cell* **62,** 1073–1085 (1990).
47. McKusick, V. A. in *Mendelian Inheritance in Man* 916–917 (Johns Hopkins Univ. Press, 1990).
48. Greenberg, F., Elder, F. F. B., Haffner, P., Northrup, M. & Ledbetter, D. M. *Am. J. hum. Genet.* **43,** 605–611 (1988).

ACKNOWLEDGEMENTS. We thank M. Allen, D. Harris, C. Lenz, E. Nakashima, R. Puryear and S. Tamowski for technical assistance, M. L. Kirby and E. M. Hammond for examining hearts from the *hox-1.5* mice, and D. Bramble for discussions.